

Development of an Optically-pumped Cesium Standard at the Aerospace Corporation

Dr. Yat C. Chan
Electronics Technology Center
The Aerospace Corporation
Los Angeles, CA

Abstract

We have initiated a research program to study the performance of compact optically-pumped cesium (Cs) frequency standards, which have potential for future timekeeping applications in space. A Cs beam clock apparatus has been assembled. Basic functions of the frequency standard have been demonstrated. Clock signals are observed with optical pumping schemes using one or two lasers. With two-laser pumping, we are able to selectively place up to 80% of the atomic population into one of the clock transition states. The observed pattern of the microwave clock signal indicates that the velocity distribution of the Cs atoms contributing to the microwave signal is beam-Maxwellian. Thus, in the optically-pumped Cs frequency standards, the entire Cs population in the atomic beam could be utilized to generate the clock signals. This is in contrast to the conventional Cs beam standards where only ~1% of the atoms in the beam are used. More efficient Cs consumption can lead to improved reliability and increased useful lifetime of the clock. Our preliminary results are summarized in this paper.

INTRODUCTION

There has been considerable interest in the use of optical methods for state preparation and clock signal detection in the Cs frequency [1],[2],[3]. Elimination of the state selection magnets in the frequency standard could significantly reduce the frequency biases which are magnetic dependent such as those due to the Majorana transitions and the distributed cavity phase-shifts. Reductions of the magnitudes of these effects can lead to a clock in which the stability and the accuracy are greatly improved over current designs. Potentially, an accuracy of 1 part in 10^{14} is achievable in optically-pumped Cs beam frequency [4].

In a conventional Cs beam clock, the state selection magnets select only a small group of Cs atoms with a narrow velocity spread and an appropriate hyperfine energy state, such that only ~1% of the total atoms in the beam contributes to the observed clock signal. Such inefficient use of the Cs has adverse effects on the lifetime of the beam clock, since the major cause of failures in the compact Cs beam clocks is due to the exhaustion of Cs in the oven. Optical excitation with the laser beam perpendicular to the atomic beam is insensitive to the velocity of Cs atoms along the atomic beam axis. Additionally, optical pumping schemes using two lasers can concentrate nearly the entire Cs population into one of the clock transition states. Thus, all of the Cs atoms in the beam could be utilized. This could translate into a larger clock signal and more efficient Cs consumption resulting in increased reliability and useful lifetime of the clock.

We have initiated a research program to gain familiarity with the optical pumping techniques in Cs frequency standards. In particular, we are interested in studying the stability and reliability of compact frequency standards which have potential for future timekeeping applications in space. Hopefully, these investigations will lead to improved performance in compact optically pumped Cs standards (OPCS). Our preliminary observations are summarized in this paper.

EXPERIMENTAL SECTION

A schematic diagram for our experimental setup is presented in Fig. 1. Our Cs beam apparatus consists of four main sections: a Cs source, a pumping chamber, a microwave region and a detection chamber. Separations between the Cs oven and the pumping and detection regions are 64 and 132 cm, respectively. The vacuum chamber is evacuated to $\sim 10^{-7}$ Torr by a 120 l/s ion pump. In the pumping chamber and the detection chamber, three optical windows are mounted perpendicular to the atomic beam providing access for the laser beams and for the detection of emission signals. Effusion of Cs atoms from the Cs oven through a 2.4 mm diameter opening into the vacuum chamber forms an atomic beam. The temperature of the Cs oven is maintained at 120 °C during the experiment. A graphite diaphragm with a 2.5 mm diameter aperture is placed 7.5 cm from the oven to reduce the beam divergence and the Cs background.

A single layer of 1.5 mm thick mu-metal provides shielding against interferences from ambient magnetic fields. Stray magnetic fields inside the chamber are less than 2.5 mG. A dc magnetic field (C-field), perpendicular to the atomic beam, is produced inside the magnetic-shielding chamber by four current-carrying copper rods placed 4 cm apart. Inhomogeneity of the C-field is less than 5 mG across the cross section of the atomic beam. A compact Ramsey-type microwave cavity of commercial design is mounted in the microwave chamber. Separation between the two, 1 cm long arms of the U-shaped microwave cavity is 12 cm. The cross sectional area of the cavity is $\sim 15 \text{ mm}^2$ allowing approximately 2×10^{10} atoms/s to be interrogated by the microwave field. The output of a temperature stabilized VCXO, operating at 143 MHz, is multiplied 64 times to provide the required microwave radiation.

Diode lasers are used for both optical pumping and state detection. The lasers are tuned to the Cs D₂ transition frequencies by controlling both the laser heat-sink temperatures and the laser injection currents. In order to keep the laser frequency on resonance with the Cs atomic transitions throughout the experiment, the laser frequencies are locked onto the selected atomic transitions through an electronic feedback technique using the fluorescence signals provided by a photodiode detector in the pumping region. As a part of the electrical feedback technique, the injection currents of the lasers are modulated by small ac signals oscillating at 700 or 1000 Hz. The modulations increase the effective linewidths of the lasers to ~ 80 MHz. Depending on the individual laser, laser powers available vary from 2 to 8 mW.

Fluorescence signals in the detection region are detected by a cooled GaAs photomultiplier tube. The signals are amplified by an electrometer with ~ 1 s time constant.

RESULTS

(A) Hyperfine Pumping

An energy level diagram for the Cs D₂ transitions is given in Figure 2. Selection rules for the optical transitions are $\Delta F = 0$ or ± 1 , (F is the total angular momentum of a state, nuclear plus electronic) such that six optical transitions between the ground 6²S_{1/2} state and the excited 6²P_{3/2} state are permitted. The selection rules also depend on the polarization of the excitation source. When the polarization of the laser is perpendicular to the magnetic field, σ -excitations will be induced, such that the allowed optical transitions are $\Delta M = \pm 1$ (M describes the projection of F onto the direction of the magnetic field). For the π -excitations, polarization of the laser is aligned parallel with the C-field, and the allowed transitions are $\Delta M = 0$, with the exception that $M = 0 \rightarrow M' = 0$ (primes indicate the angular momentum of the excited state) is forbidden when $\Delta F = 0$.

Transitions including: $F = 4 \rightarrow F' = 4$; $F = 4 \rightarrow F' = 3$; $F = 0 \rightarrow F' = 3$; $F = 30 \rightarrow F' = 4$ are known as the pumping transitions. With these pumping excitations, Cs population may be transferred from one of the ground electronic state hyperfine levels into the other, consequently give rise to the hyperfine pumping. For the cycling transitions, $F = 4 \rightarrow F' = 5$ and $F = 3 \rightarrow F' = 5$, the only decay pathway for the excited atoms upon excitation is returning to their original ground hyperfine levels, therefore they are not useful for optical pumping. Fig. 3a shows a fluorescence spectrum collected at the detection chamber when the frequency of a probe laser was scanned over the d₂ transitions of Cs around 852 nm. All six allowed optical transitions were observed. Fig. 3b shows a similar emission spectrum, when a second laser was tuned to the $F = 3 \rightarrow F' = 3$ transition and intersected the atomic beam in the pumping region. Emission signals corresponding to the $F = 3 \rightarrow F' = 2, 3, 4$ transitions disappeared completely. This is due to the complete removal of the $F = 3$ population by hyperfine pumping in the pumping region. Similar hyperfine pumping effects were observed with the other pumping excitations. These observations confirm that near complete population transfer from one hyperfine state into the other can be achieved by optical pumping using diode lasers.

(B) Optical Pumping with One Laser

In our one-laser experiment, the main laser beam was used for optical pumping in the pumping chamber. A fraction of the laser beam was diverted into the detection chamber for state detection. Hyperfine pumping was induced by tuning the laser onto one of the pumping transitions. When the microwave source fed to the Ramsey-cavity was off, emission signals observed in the detection region consisted mainly of scattered laser light and a small fluorescence signal from the unpumped Cs atoms. When the microwave frequency matched the Cs hyperfine transition frequencies, transitions between the two hyperfine states would be induced among the Cs atoms passing through the microwave cavity. This resulted in a change in the emission signals observed in the detection chamber. Fig. 4a shows the microwave spectrum with the $F = 3 \rightarrow F' = 3$ σ pumping scheme (3-3 σ), where the notation σ (or π) describes the polarization of the pumping laser with respect to the C-field as discussed in the previous section. The microwave spectrum consists of seven transitions. The (0-0) 'clock' transition, which couples the $F=3, M=0$ and $F=4, M=0$ states, shows the characteristic interference structures. The halfwidth of the central Ramsey peak is approximately 1 KHz. Such interference structures, however, were not observed in the other microwave transitions. This could be due to the fact that interference structures on these magnetic sensitive transitions were washed out by the inhomogeneity of the C-field. This result suggests that an improvement in the uniformity of the C-field is desirable.

State preparation involving $3-3 \pi$ and $4-4 \pi$ pumping are important components of the two-laser pumping techniques for putting all of the Cs atoms into one of the clock transition states. Fig. 4b shows the microwave spectrum when the $3-3 \pi$ pumping scheme is employed. By rotating the laser polarization 90 degrees, $3-3 \sigma$ excitation can be used for detection. Due to the selection rules, the $M = 0 \leftrightarrow M' = 0$ transition is forbidden in the $3-3 \pi$ excitation, such that population in the $F=3, M=0$ level will not undergo excitation. The unpumped Cs atoms contributed to a large background signal and an increased noise level in the spectrum. Figure 4c gives the microwave spectrum observed when the $4-4 \sigma$ pumping scheme is used.

Figure 4d compares the measured relative intensities of the microwave transitions resulting from the $3-3 \sigma$ excitation scheme of Fig. 4a with the calculated values. The calculated values are obtained from the matrix elements for the seven hyperfine transitions, assuming that the populations of the magnetic sublevels in the unpumped hyperfine state are equal and the pumped hyperfine state is completely depopulated. Excellent agreement between the experimental results and the calculated values indicates that the seven sublevels ($M = 0, \pm 1, \pm 2, \pm 3$) in the $F=4$ hyperfine state are indeed equally populated. In certain pumping schemes, due to the selection rules and the differences in the transition probabilities for the D_2 lines among the Zeeman sublevels, alignment of the atomic population (i.e. nonuniform population of Zeeman sublevels) could be created. Relative intensities of the microwave signals in Fig. 4b and 4c are compared with the calculated values in Fig. 4e and 4f, respectively. It is clear that levels with the high magnetic quantum numbers, M , are favored when $3-3 \pi$ pumping is employed. In the case of the $4-4 \sigma$ scheme, levels with $M = \pm 2$ are preferred.

(C) Two-Laser Experiment

In this experiment, two lasers are used in an attempt to concentrate all of the Cs population into one of the two clock transition Zeeman sublevels by using both the hyperfine and Zeeman optical pumping techniques. Experimental arrangements were similar to those used in the one-laser experiment with the exception that an additional pumping laser was used for Zeeman pumping. Fig. 5a shows the microwave spectrum with $4-4 \pi$ and $3-3 \sigma$ pumping, and $3-3 \sigma$ detecting. Signal for the (0-0) 'clock' transition was greatly increased compared to the one-laser pumping experiment at the expense of the other microwave transitions. With this arrangement, we were able to concentrate $\sim 80\%$ of the atomic population into the $F=4, M=0$ level. Fig. 5b shows the atomic population distribution among the magnetic sublevels of the $F=4$ hyperfine states. About 7% atomic population remained in the $F=3$ state, which contributed to the increased noise figure in the spectrum. With $4-4 \sigma$ and $3-3 \pi$ pumping, $\sim 70\%$ Cs atoms were concentrated into the $F=3, M=0$ level.

At low values of magnetic field strength, optical pumping efficiencies involving s -transitions will be reduced. This is due to the creation of $\Delta M = \pm 2$ Zeeman coherences in the Cs ground state [5]. Thus, it would be undesirable to use σ -transitions in optically pumped frequency standards when a low C-field is needed. Figure 6 shows the result of our measurements of the % population concentrated in the $F=3, M=0$ clock state using the $3-3 \sigma$ and $4-4 \pi$ two-laser pumping scheme. Below 70 mG, the neighboring microwave transitions interfered with the clock signal, thus no measurement was conducted below that value of magnetic field. No evidence for the reduction of pumping efficiency was observed over the C-field range of 70 to 1500 mG.

(D) Velocity Distribution in the Atomic Beam

Figure 6 shows the Ramsey-Rabi signal of the (0-0) 'clock' transition obtained in an one-laser experiment. 3-3 σ excitation was used for both pumping and detecting. Calculated values of the clock signal, assuming that the velocity distribution in the Cs beam is beam-Maxwellian, are plotted as circles in the figure. Agreement between the experimental and the calculated values is satisfactory. This indicates that the velocity distribution of atoms contributing to the microwave signal is beam-Maxwellian, with a temperature consistent with that of the oven source.

CONCLUSIONS

We have established a facility for studying compact optically pumped Cs frequency standards. Basic functions of the atomic clock system have been demonstrated. In the two-laser experiment, we are able to concentrate ~80% of the atomic population in one of the 'clock' transition states. The velocity distribution of the Cs atoms in the atomic beam are found to be approximately beam-Maxwellian, which indicates that the optical state preparation and detection methods used in the OPCS are insensitive to the velocity of Cs atoms along the atomic beam. Thus in contrast to the magnetic state selection techniques used in conventional Cs clocks, optical state preparation and detection techniques allow much more efficient uses of the atomic beam flux, which can lead to improved reliability and increased useful lifetime of the clock.

ACKNOWLEDGEMENTS

The author would like to thank Dr R. Frueholz for his many helpful discussions and encouragements. This research was sponsored by the U.S. Air Force Space Systems Division under Contract No. F04701-88-C-0089.

REFERENCES

- [1] N. Dimarcq, V. Giordano, G. Theobald and P. Cerez, *J. Appl. Phys.* **69**, 1158 (91).
- [2] S. Ohshima, Y. Nakadan, T. Ikegami, Y. Koga, R. Drullinger and L. Hollberg, *IEEE Trans. Instrum. Meas.* IM-38, 533 (89).
- [3] P. Tremblay and C. Jacques, *Phys. Rev. A*, **41**, 4989 (1980).
- [4] R. E. Drullinger, *Proc. 44th Annual Symposium on Frequency Control* 76 (1990).
- [5] V. Giordano, A. Hamel, P. Petit, G. Theobald, N. Dimarcq, P. Cerez and C. Audoin, *Proc. 43rd Annual Symposium on Frequency Control*, 130 (1989).

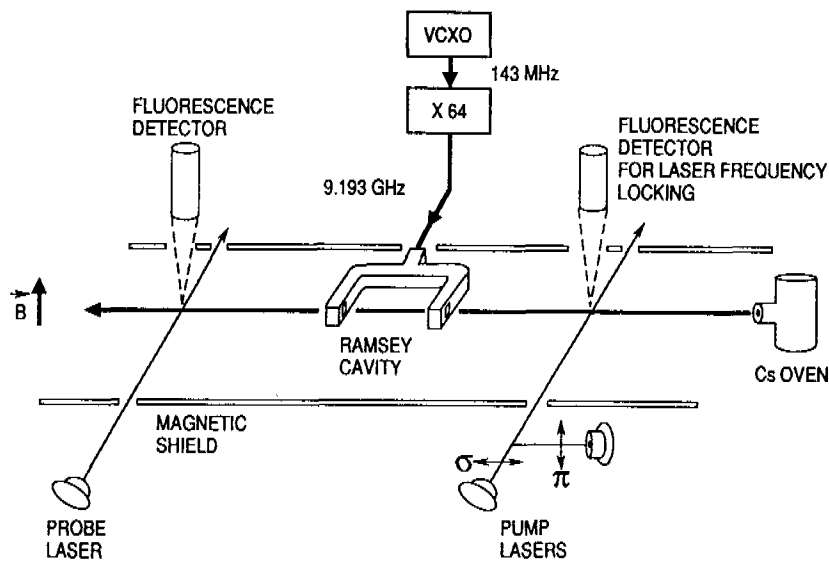


Fig. 1. Schematic representation of the optically pumped Cs frequency standard apparatus.

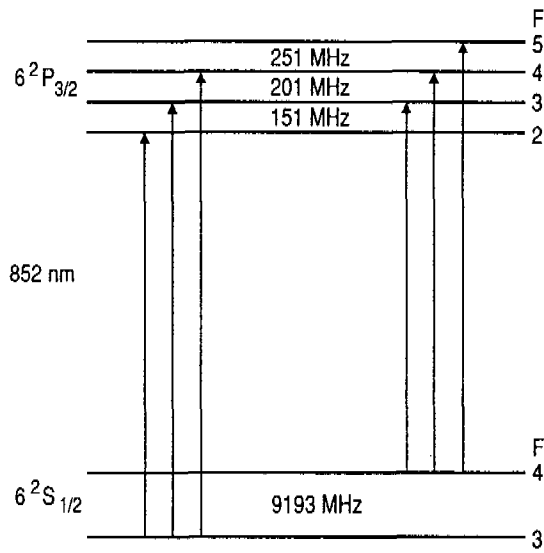


Fig. 2. Energy-level diagram for the D₂ transitions of Cs.

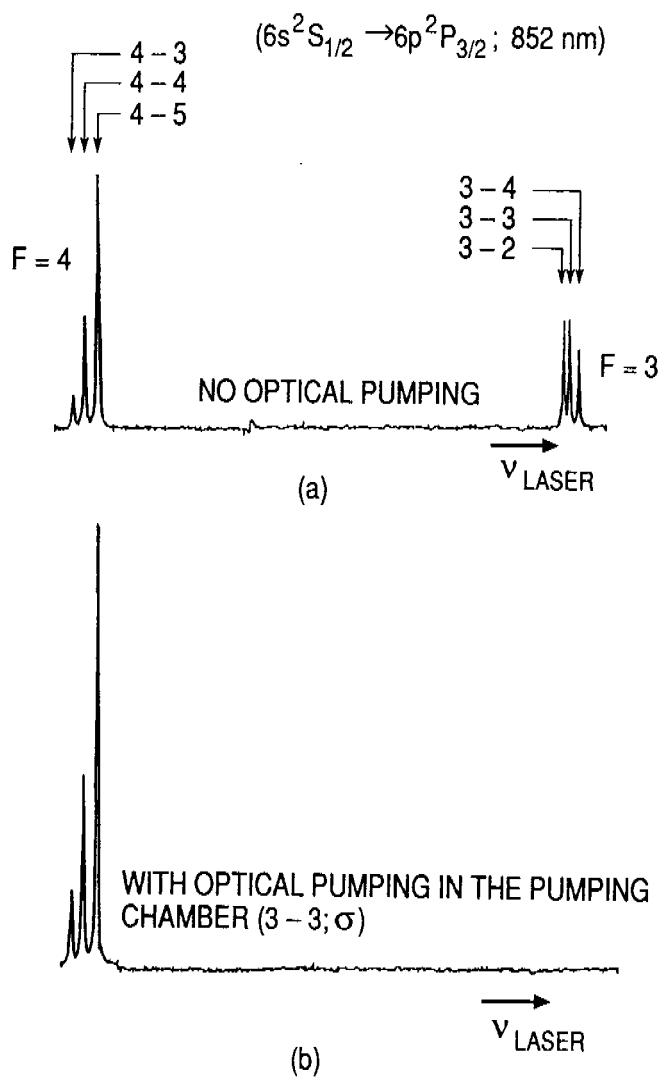


Fig. 3. Laser-induced fluorescence spectrum of the D₂ transitions of Cs at the detection chamber: (a) no optical pumping; (b) with 3-3 σ pumping in the pumping chamber.

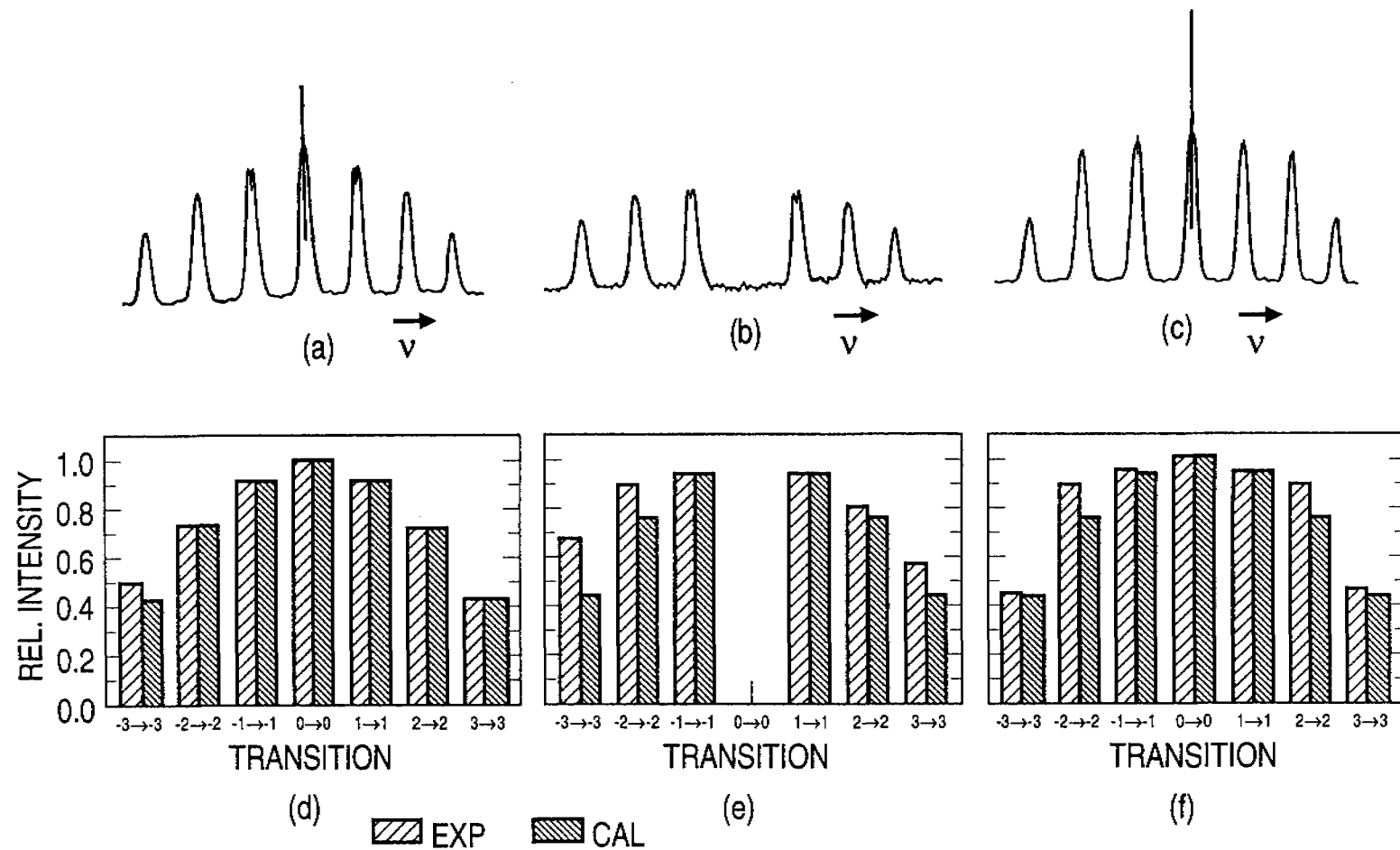
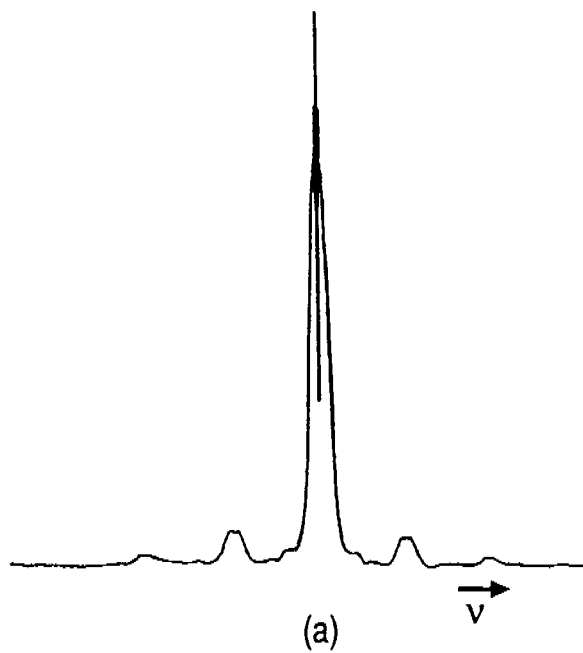
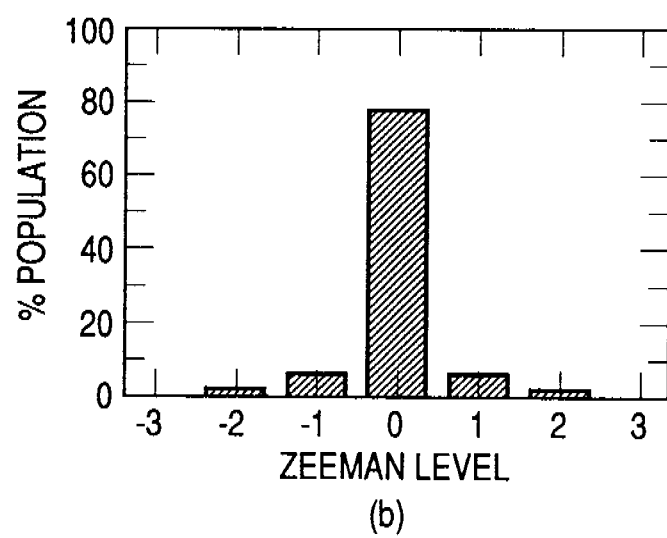


Fig. 4. (a), (b), (c) Microwave spectra of the OPCS pumped with one laser. Experimental conditions: (a) 3-3 σ pumping and detecting; (b) 3-3 π pumping and 3-3 σ detecting; (c) 4-4 σ pumping and detecting. Relative intensities of the microwave signals in (a), (b) and (c) are compared with the calculated values in (d), (e) and (f), respectively.



(a)



(b)

Fig. 5. (a) Microwave spectrum of the OPCS with the 4-4 π , and 3-3 σ pumping scheme and detected with the 3-3 σ transition. (b) Atomic population distributions among the Zeeman levels in $F=4$ level, as a result of the two laser pumping.

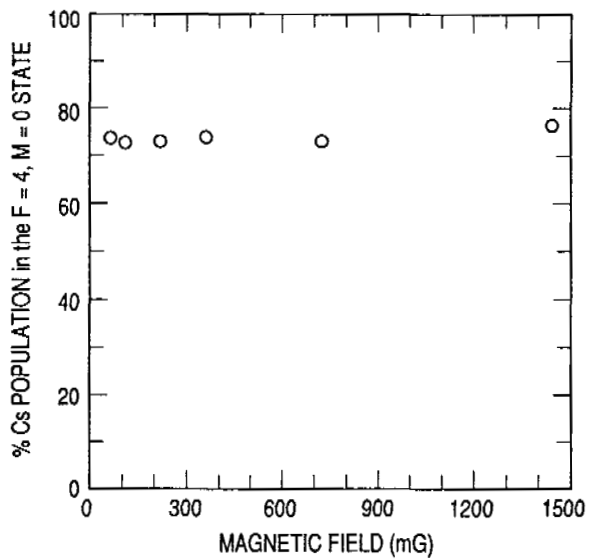


Fig. 6. Percent of atomic population concentrated in the $F=4$, $M=0$ level with two-laser pumping plotted as a function of the magnetic field. Pumping scheme is $3-3\sigma$ and $4-4\pi$ with $3-3\sigma$ detecting.

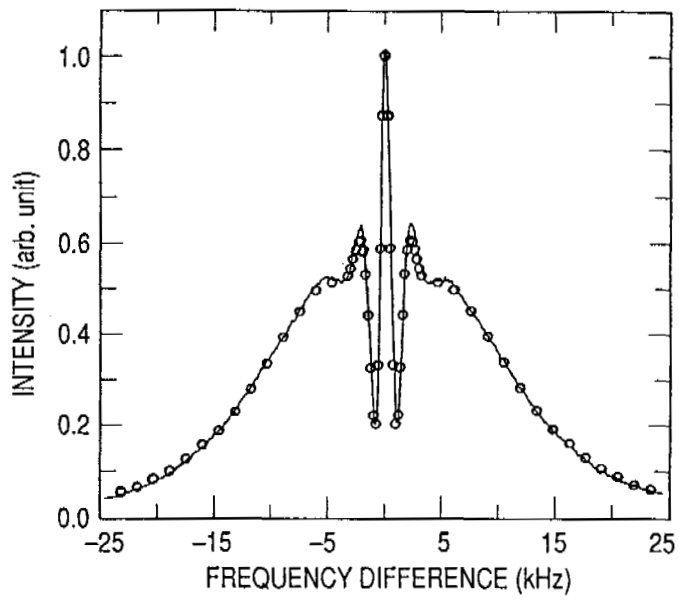


Fig. 7. Comparison of the experimental and the calculated Ramsey-Rabi structure of the (0-0) 'clock' transition. Experimental data and the calculated values are represented by the solid line and the circles, respectively.